Appl. Phys. A (2016) 122:1
DOI 10.1007/s00339-015-9525-1

Applied Physics A
Materials Science & Processing

Anti-icing properties of superhydrophobic ZnO/PDMS composite coating

Chao Yang[1] · Fajun Wang[1,2] · Wen Li[1,2] · Junfei Ou[1,2] · Changquan Li[1,2] · Alidad Amirfazli[3]

Received: 25 August 2015 / Accepted: 5 December 2015 / Published online: 15 December 2015

Abstract We present the excellent anti-icing performance for a superhydrophobic coating surface based on ZnO/polydimethylsiloxane (ZnO/PDMS) composite. The superhydrophobic ZnO/PDMS coating surface was prepared by a facile solution mixing, drop coating, room-temperature curing and surface abrading procedure. The superhydrophobic ZnO/PDMS composite coating possesses a water contact angle of 159.5° and a water sliding angle of 8.3° at room temperature (5 °C). The anti-icing properties of the superhydrophobic coating were investigated by continuously dropping cold-water droplets (about 0 °C) onto the pre-cooled surface using a home-made apparatus. The sample was placed at different tilting angle (0° and 10°) and pre-cooled to various temperatures (−5, −10 and −15 °C) prior to measure. The pure Al surface was also studied for comparison. It was found that icing accretion on the surface could be reduced apparently because the water droplets merged together and slid away from the superhydrophobic surface at all of the measuring temperatures when the surface is horizontally placed. In addition, water droplet slid away completely from the superhydrophobic surface at −5 and −10 °C when the surface is tilted at 10°, which demonstrates its excellent anti-icing properties at these temperatures. When the temperature decreased to −15 °C, though ice accretion on the tilted superhydrophobic coating surface could not be avoided absolutely, the amount of ice formed on the surface is very small, which indicated that the coating surface with superhydrophobicity could significantly reduce ice accumulation on the surface at very low temperature (−15 °C). Importantly, the sample is also stable against repeated icing/deicing cycles. More meaningfully, once the superhydrophobic surface is damaged, it can be repaired easily and rapidly.

1 Introduction

Ice formation and accumulation on key parts of many essential infrastructures such as aviation, power lines, insulators, wind turbine blades and helicopter blades will lead to severe accidents, damaging problems, economic losses and serious safety issues [1–5]. For example, ice formation on helicopter blades results in the change of the airfoil shape and the degradation of performance because of blade vibration, increased drag, increased torque and decreased lift [4, 6]. Ice accretion on insulators and overhead transmission lines in transmission system cause serious accidents such as tower toppling, wire breakage and flashover, as reported in Eastern Canada of 1998 and in South China of 2008. The statistics indicated that the 2008 ice disaster in South China led to an economic loss of 7.9 billion US dollars (53.7 billion China Yuan) in transmission system [1, 2]. Various methods and technologies have

Electronic supplementary material The online version of this article (doi:10.1007/s00339-015-9525-1) contains supplementary material, which is available to authorized users.

✉ Fajun Wang
jjbxsjz@foxmail.com

[1] School of Materials Science and Engineering, Nanchang Hangkong University, Nanchang 330063, People's Republic of China

[2] Key Laboratory for Microstructural Control of Metallic Materials of Jiangxi Province, Nanchang Hangkong University, Nanchang 330063, People's Republic of China

[3] Department of Mechanical Engineering, University of Alberta, Edmonton, AB, Canada

been used to resolve the problem of ice accumulation, such as thermal deicing, electric deicing, mechanical deicing and the use of deicing fluid [7–11]. However, the disadvantages of these deicing methods are obvious, ranging from expensive, energy consumption to environmentally harmful. Therefore, developing of cheap and environmentally friendly materials or techniques for insulators, aviations, helicopter blades, etc., is highly desirable.

It is well known that water droplets freeze and form ice on solid surface when the surface temperature is below 0 °C [12, 13]. If water adhesion on solid surface could be avoided, the ice formation on the surface could be eliminated. Superhydrophobic surfaces possess extremely high contact angle (CA, >150°) for water as well as very low sliding angle (SA, <10°) [14–16]. Water droplets on the superhydrophobic surface are instable and easy to leave the surface when the surface is slightly tilted or blew by natural wind due to the low SA of the surface [17–19]. Based on these considerations, superhydrophobic coatings or surfaces have received considerable attention due to their suppositional anti-icing/icephobic characteristic during the last decades [20–24]. For example, Wang et al. [24] prepared four surfaces based on Al substrate with different surface wettabilities, i.e., superhydrophilic, hydrophilic, hydrophobic and superhydrophobic surfaces, by a two-step etching and surface modification method. Overcooled water left the superhydrophobic surface of Al under a relative humidity of 90 % and a temperature of −10 °C. Cao et al. [23] prepared superhydrophobic surface based on particle/polymer composite coatings and investigated the anti-icing properties by using supercooled water in laboratory as well as in practical freezing conditions. The superhydrophobic coating on Al substrate exhibited effective anti-icing properties in comparison with the uncoated Al surface. In addition, the results also indicated that the anti-icing performances of the superhydrophobic composites were influenced not only by the superhydrophobicity but also by the particle sizes. Guo et al. [8] fabricated ZnO nanohair structures on stainless steel plate via a hydrothermal synthesis method. After being modified with FAS-17, the ZnO surface exhibited superhydrophobicity. Water droplets on the surface delayed to freezing for a long time larger than 185 min. Though anti-icing/icephobic performance of various superhydrophobic coatings and surfaces has been successfully demonstrated, the aging problem and mechanical stabilities of these surfaces against normal contact and repeated freezing and thawing cycles have not been investigated yet.

In this work, we fabricated superhydrophobic ZnO/PDMS composite coating via a simple method. The ZnO particles were first modified with 1-dodecanethiol (DT) to improve the surface hydrophobicity of the particles. Then, the modified ZnO particles were mixed with PDMS in hexane and drop-coated on Al sheet. After curing at room temperature, the ZnO/PDMS composite was abraded with sandpaper to generate superhydrophobicity [25, 26]. The anti-icing and/or icing performances of the horizontal and tilted samples were studied at various temperatures of −5, −10 and −15 °C. The superhydrophobic ZnO/PDMS composite coating could reduce ice accumulation on the horizontal surface at all of the measuring temperatures and on the tilted surface at −15 °C. In addition, the tilted surface could completely eliminate ice formation on the superhydrophobic surface of ZnO/PDMS composite at −5 and −10 °C. Importantly, the superhydrophobicity of the composite is stable against abrading and repeated icing/deicing cycles. Furthermore, the superhydrophobicity of the ZnO/PDMS composite can be restored quickly anytime anywhere. Moreover, the fabrication method could be extended to other particle/polymer composite system. The findings demonstrate that the superhydrophobic surface of ZnO/PDMS composite could be used in future anti-icing coatings.

2 Experimental

ZnO particles were purchased from Shanghai Chaowei Nanotechnology Co., Ltd (China). DT was purchased from Sigma-Aldrich. Polydimethylsiloxane (PDMS) was obtained from Hubei WD Silicon Co., Ltd (China). Tetraethoxysilane (TEOS) and dibutyl tin dilaurate were obtained from Shanghai Silicon Mountain Co., Ltd (China). Hexane was purchased from Xiya Chemical Reagent Co., Ltd. Sandpaper (320 #) was obtained from 3 M Co., Ltd (China).

The surface modification of ZnO particles was achieved as per the reported method [27, 28]. Typically, 10 g of ZnO particles was suspended in 100 mL of hexane under ultrasonification for about 10 min. Then, 20 μL of DT was quickly added into the suspension. The suspension was magnetically stirred for about 30 min and aged overnight. Finally, the modified ZnO particles were obtained by centrifugation from hexane suspension. The ZnO/PDMS composite coatings were prepared by a drop-casting method. Briefly, ZnO particles, PDMS and hexane were mixed in a planetary ball mill for 2 h to form a homogeneous suspension. Then, TEOS (curing agent) and dibutyl tin dilaurate (accelerating agent) were added into the suspension. After continuous ball-milling for another 10 min, the suspension was drop-coated onto Al sheets. The ZnO/PDMS composite coatings were obtained after being cured at room temperature overnight. The superhydrophobic ZnO/PDMS composite coatings were prepared using a simple abrading method as reported in the literatures [25, 26].

The Fourier transform infrared (FTIR) spectra were measured using an infrared spectrometer (VERTEX 70, Bruker, Germany). The surface microstructures were obtained on a field emission scanning electron microscope (FESEM, FEI, Nova NanoSEM 450). Water CAs and SAs were obtained using a CA measurement apparatus (Krüss DSA 100, Germany) according to the reported method [25]. The icing behaviors of the superhydrophobic coating surfaces were recorded using a home-made apparatus (see Fig. 1). Cold water (about 0 °C) was added dropwise onto the surface of sample. The sample was stuck to the surface of a thermoelectric cooler (TC) using a thermally conductive adhesive. The water droplet was added onto the sample surface every 2 s. The sample was pre-cooled for about 10 min prior to measuring. The tilting angle of the sample could be adjusted form 0° to 90° by using the tilting stage. The distance from the bottom of the dropping funnel to the sample surface is fixed at about 5 cm. Once the falling droplet makes contact with the sample surface, it either sticks to the surface or rolls away from the surface, which exhibits different icing behaviors of the surface. The icing behaviors were observed and recorded by a digital camera (EOS 7D). The ambient temperature is 5 °C, and the relative humidity is about 75 % for all of the icing behavior measurements.

3 Results and discussion

Figure 2 shows the FESEM image of the as-received ZnO particles. One can see that the ZnO particle shows mainly square-like shapes with typical size ranging from several hundred nanometers to about 1 micrometer. Figure 3 shows the FTIR spectra of the ZnO particles before and after DT modification. Two new peaks at 2933 and 2857 cm^{-1} were clearly observed from the FTIR spectrum of the modified ZnO particles, which is attributed to the stretching vibration of CH_3 and/or CH_2. The result

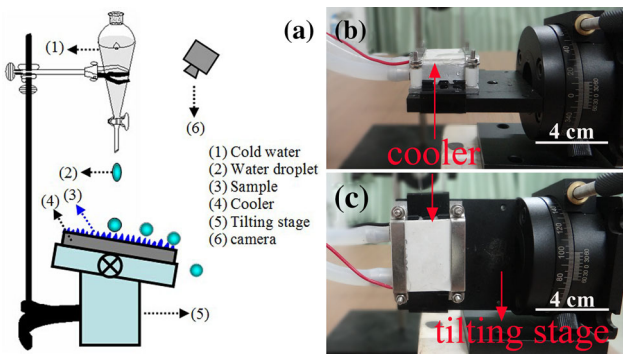

Fig. 1 **a** Illustration for the measurement of icing behaviors using a home-made apparatus; **b** cooler was horizontally placed; **c** cooler was vertically placed

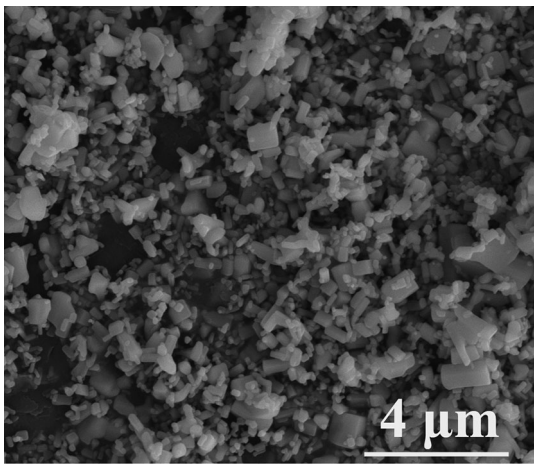

Fig. 2 FESEM image of the as-received ZnO particles

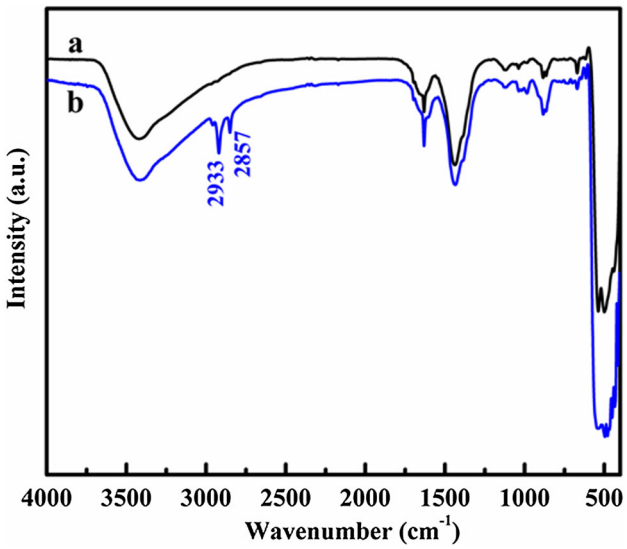

Fig. 3 FTIR spectra of ZnO particles; **a** as-received ZnO particles; **b** modified ZnO particles

indicates that the groups of $–C_{12}H_{25}$ were successfully self-organized on the surface of the ZnO particles. The existing of surface DT on the ZnO particles could also be proved by wettability measurement. Figure 4a, b shows the shapes of water droplets on the surface of 5 g ZnO particles before (Fig. 4a] and after (Fig. 4b) DT modification. Apparently, water wets the unmodified ZnO particles easily when it makes contact with the particles (Fig. 4a). However, water droplets either show ball-like shapes on the modified ZnO particles or roll away from the surface (Fig. 4b), which demonstrates the highly hydrophobicity of the ZnO particles.

Figure 5 shows the influence of ZnO weight fraction on water CAs and SAs of the ZnO/PDMS composites. Overall, the CAs increase and the SAs decrease with increasing ZnO weight fraction. Particularly, the ZnO/PDMS composite

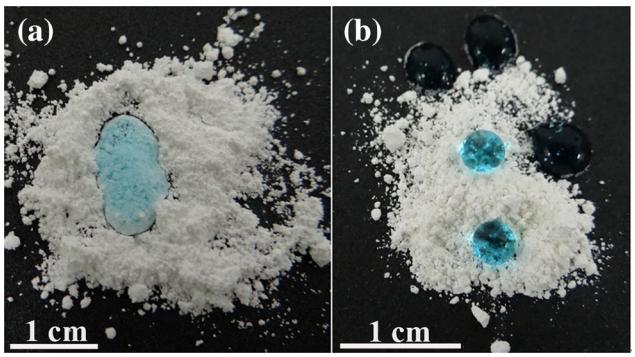

Fig. 4 Digital pictures of water droplets added on the surface of ZnO particles; **a** as-received ZnO particles; **b** modified ZnO particles

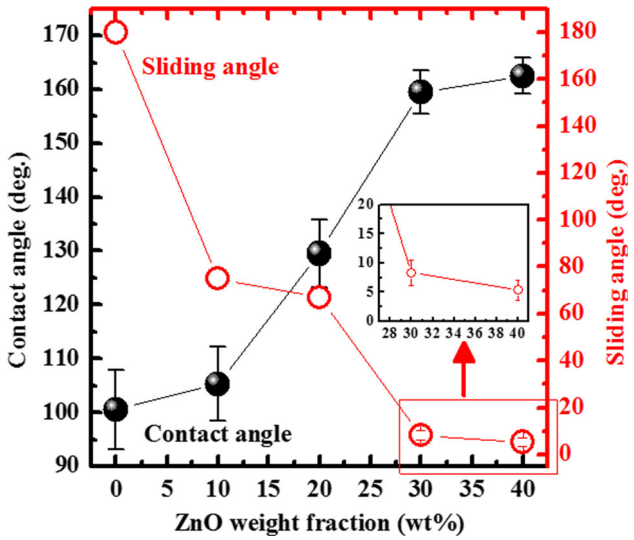

Fig. 5 Influence of ZnO weight fraction on water CAs and SAs of the ZnO/PDMS composites. The *inset* shows the magnified image

begins to exhibit superhydrophobicity when ZnO content is equal to 30 wt%, i.e., with a CA of 159.5° and a SA of 8.3° (see inset). Further increasing ZnO content to 40 wt% is beneficial to improve the superhydrophobicity of the composite. However, both the increase in CA and the decrease in SA are not significant. On the contrary, high filler content on the PDMS matrix results in the increase in brittleness of the ZnO/PDMS composite. Hence, the superhydrophobic ZnO/PDMS composite with ZnO content at 30 wt% was chosen for the characterization of its icing behavior.

The microstructures of the ZnO/PDMS composite surface with different ZnO weight fraction are shown in Fig. 6a–f. From the low-magnification images in Fig. 6a–c, the surfaces exhibit irregular topographies, with lots of grooves and protrusions spreading all over the surfaces. The rough microstructures are attributed to the surface abrading process. The ZnO particles homogeneously distribute throughout the surfaces without apparent agglomeration, as can be seen from the high-magnification images in Fig. 6d–f. The surface wettability of the ZnO/PDMS composite (30 wt% ZnO) is shown in Fig. 7b. The pure Al sheet surface is also investigated for comparison (Fig. 7a). One can see that the pure Al surface is hydrophilic (contact angle = 84.3°) and water droplet sticks firmly to the surface even when the surface is vertically placed (not shown in this figure). The surface morphology of pure Al surface is shown in supporting information [SI, Figure S1]. A relatively smooth surface of Al [Figure S1(a)] and some micrometer scratches [Figure S1(b)] can be observed in the FESEM images in comparison with the surface of ZnO/PDMS composite. In contrast, water droplet showing ball-like shape sits on the surface of the composite (Fig. 7b). The composite possesses a high CA of 159.4° and a low SA of 8.3° for water [also see Fig. 6], which demonstrates the superhydrophobicity of the ZnO/PDMS composite.

The freezing processes of water on the hydrophilic Al surface (denoted as Al hereafter) and the superhydrophobic surface of ZnO/PDMS composite (denoted as ZnO/PDMS hereafter) were systematically studied. The water droplets fall onto the Al surface, adhere to the surface and gradually freeze at different temperatures of −5, −10 and −15 °C when Al surface is horizontally placed (see Fig. 8a1–h1). The freezing speed increases with increasing temperatures. A similar phenomenon could also be observed when the Al surface is slightly inclined at 10° (see Fig. 8a2–h2). The results suggest that the Al surface does not possess the anti-icing properties. In contrast, the ZnO/PDMS composite still shows high hydrophobicity at −10 and −5 °C. Water shows spherical shapes when the falling droplets are in contact with the surface at −5° and −10°, and is apt to sliding. When the temperature decreases to −15 °C, the CA of the sample surface seems to be lower and the water adhesion can also be observed. However, water droplet does not freeze on all of the above surfaces between the temperature of −5 and −15 °C. The phenomenon that water froze quickly on Al surface while not easy to freeze on the superhydrophobic surface of ZnO/PDMS composites was mainly attributed to the difference of the thermal conductivity between Al and the composite, and the area of water droplet in contact with the surface of Al and the composite. As we know, the thermal conductivity of metal Al is significantly higher than that of the ZnO/PDMS (metal oxide/polymer) composite. Additionally, the contact area of surface water with Al substrate (hydrophilic, CA is lower) is significantly higher than it with the ZnO/PDMS composite surface (superhydrophobic, CA is larger). According to Cassie and Baxter equation [29, 30]:

$$\cos\theta_r = f_1 \cos\theta - f_2 \quad (1)$$

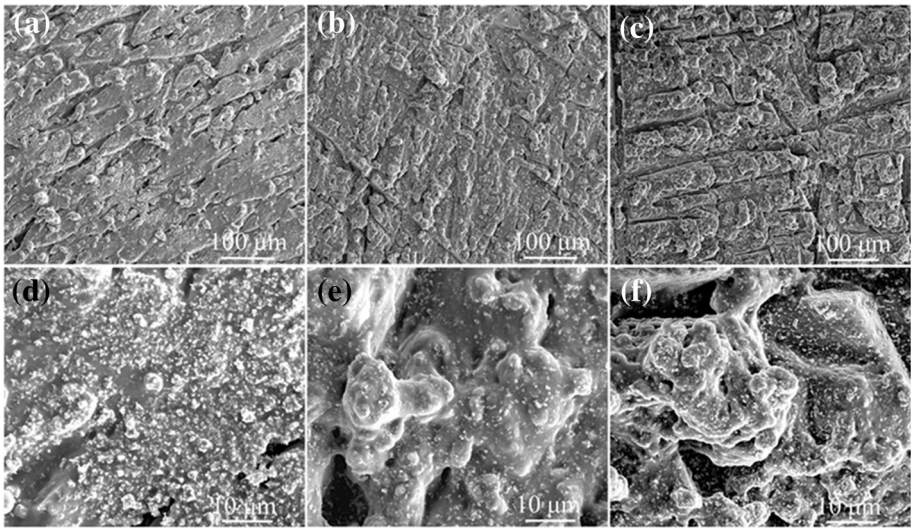

Fig. 6 SEM images of ZnO/SR composite coating. **a** and **d** ZnO weight fraction at 10 %; **b** and **e** ZnO weight fraction at 20 %; **c** and **f** ZnO weight fraction at 30 %; **a–c** at low magnification; **d–f** at high magnification

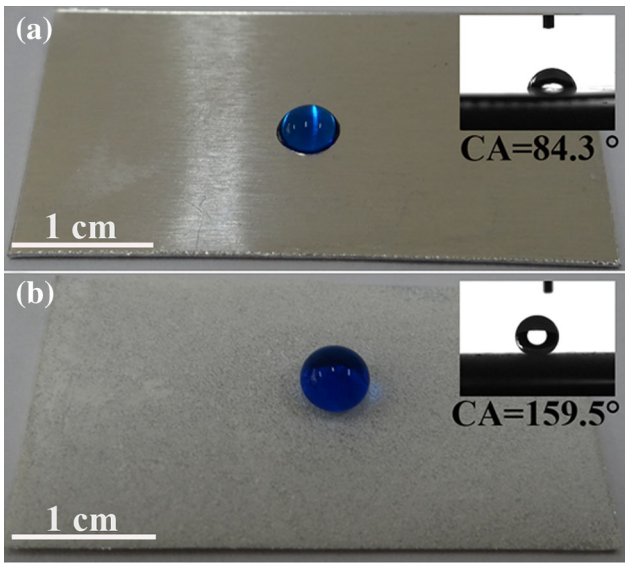

Fig. 7 Digital pictures of water droplets sit on the surfaces of the samples. (a) Al sheet; (b) Al sheet coated with superhydrophobic ZnO/PDMS composite

Here, f_1 is the fraction of solid surface in contact with water; f_2 is the fraction of air in contact with water; θ is the CA of water droplet on the smooth solid surface; and θ_r is the CA of water droplet on the rough surface of the same solid. From Eq. (1), we can calculate the value of f_1 and $f_1 = 0.127$, which means that only 12.7 % of the surface area of the ZnO/PDMS composite is in contact with water. Hence, the low thermal conductivity of the ZnO/PDMS composite combined with the low contact area with water delayed the freezing of water on the superhydrophobic surface of ZnO/PDMS composite. Moreover, when the ZnO/PDMS composite is tilted at 10°, water droplet rolls away rapidly without any residual at −10 and −5 °C. Additionally, although most of the water rolls away from the sample surface at −15 °C, adhesion of water on the surface could also be noticed occasionally.

The icing behaviors of the Al and ZnO/PDMS samples at −15 °C are depicted in Fig. 8 for the purpose of clear comparison. Figure 8a1–h1 shows the freezing process of surface water droplets on the horizontal Al substrate. Water droplet froze quickly when it made contact with the cold surface of Al (Fig. 8b1). The following water droplets continually iced up on the Al surface without sliding (Fig. 8c1–h1). When the Al surface was slightly tilted (10°), water droplet was still stuck to Al surface and froze rapidly (Fig. 8b2). The subsequent water droplets accumulated on the iced water surface and continued to freeze (Fig. 8c2–h2). Hence, the pure Al sheet could not prevent ice from accretion on its surface. Apparently, the superhydrophobic ZnO/PDMS composite surface possessed the desirable anti-icing properties, as depicted in Fig. 8a3–h3 and a4–h4. When the superhydrophobic surface is horizontally placed, the first water droplet formed ball-like shape on the surface without freezing (b3). The following water droplets also showed spherical shape sitting on the surface or occasionally merged together to form large droplet (Fig. 8c3–g3). It was noted that either the small water droplet (Fig. 8b3–d3) or the merged large water droplet (Fig. 8e3–g3) did not freeze. Importantly, the merged big water droplet spontaneously slid away from the surface, which could apparently reduce the volume of the surface water, consequently reducing the amount of ice accumulation on the surface (Fig. 8h3). More importantly, when the superhydrophobic surface is tilted at 10°, water droplets rolled away fast from the surface (Fig. 8a4–c4). Occasionally, the water droplet adhered to the surface without rolling (d4). However, it could be taken away by

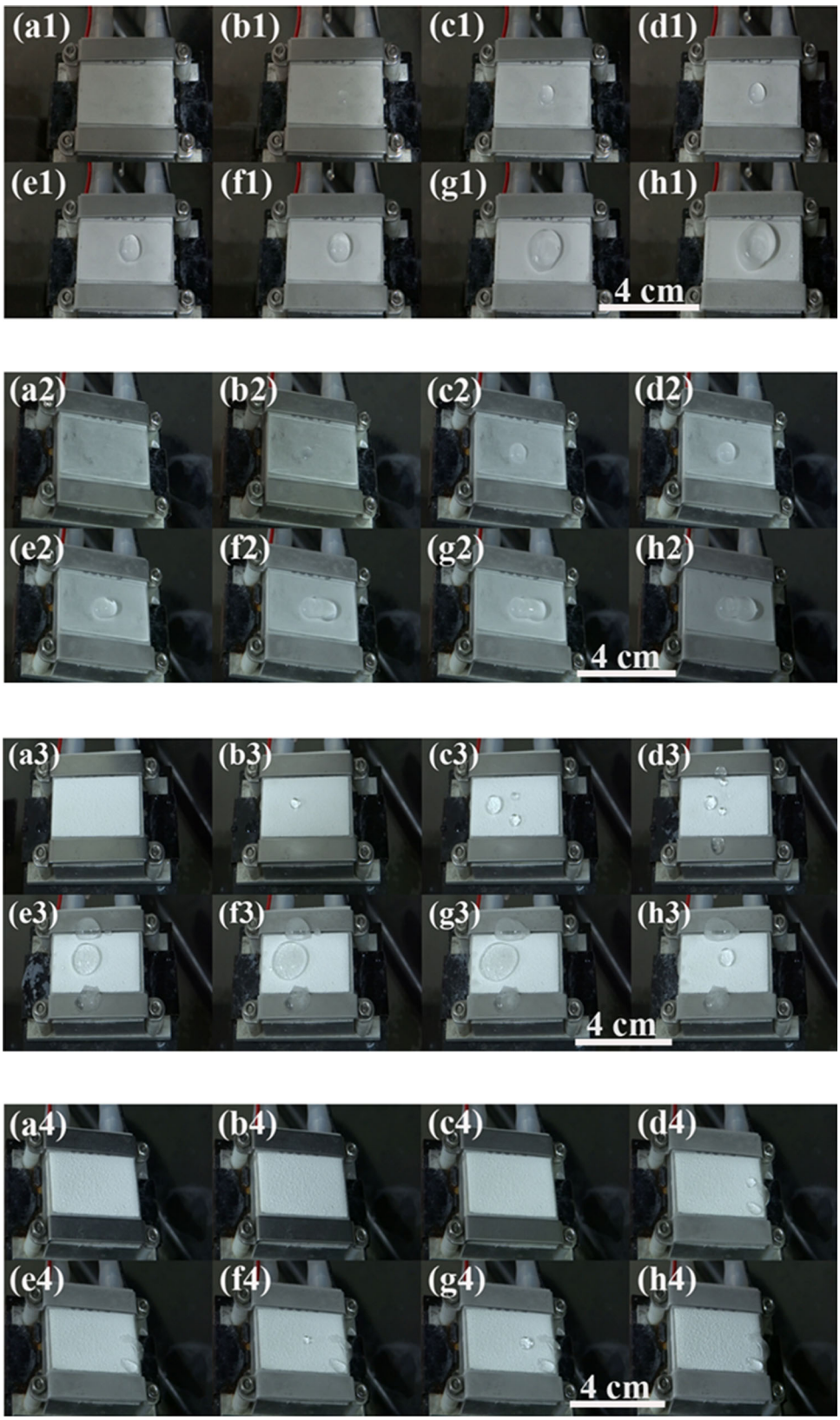

Fig. 8 Icing and/or anti-icing properties of different samples at −15 °C; **a1–h1** horizontally placed Al sheet; **a2–h2** tilted Al sheet; **a3–h3** horizontally placed superhydrophobic ZnO-SR composite; **a4–h4** tilted superhydrophobic ZnO/SR composite; **a1–a4**: at 0 s; **b1–b4**: at 1 s; **c1–c4**: at 11 s; **d1–d4**: at 21 s; **e1–e4**: at 41 s; **f1–f4**: at 71 s; **g1–g4** at 131 s; **h1–h4**: at 161 s, respectively

the following water (d4, e4). Finally, after the measuring period of about 161 s, only a small amount of ice formed on the bottom of the surface (h4).

The influence of both temperature and tilting angle on the icing behaviors of the pure Al and the superhydrophobic ZnO/PMDF surfaces was summarized in SI

[Figure S2 and S3]. The figures were obtained by taking photos after continuously dropping water onto the sample surface for about 3 min. It is clearly observed in Figure S2 that ice always froze on the pure Al surface at temperatures from −5 to −15 °C whether the surface is horizontally placed or slightly tilted. Comparatively speaking, the superhydrophobic ZnO/PDMS surface exhibits much better anti-icing properties. As shown in Figure S3, water freezing could not be observed on the surface of the superhydrophobic sample when the surface is horizontally placed even at a low temperature of −15 °C after 3 min [Figure S3 (c)]. Water slid on the surface and left the surface slowly, which results in the reduction the surface water accumulation on the sample surface. Hence, the possibility of subsequently occurred ice formation on the surface should be remarkably reduced. However, ice still formed on the interface between the ZnO/PDMS composite and the cold metal fastener [see Figure S3(a)–(c)] when the emerged big water droplet slid toward the fastener and eventually captured by the fastener, which could be attributed to the high adhesion force between water and the fastener (stainless steel material, not superhydrophobic). In addition, when the ZnO/PDMS composite sample is tilted at 10°, ice accretion on the surface could be completely avoided at −10 and −5 °C [see Figure S3(b) and (c)]. This phenomenon could be interpreted by the superhydrophobicity of the ZnO/PDMS composites. Superhydrophobic surfaces exhibited very high CA (>150°) and simultaneously very low SA (<10°) for water. As a result, water droplets rolled away the surface composite rapidly because the surface is tilted at 10°. At the measuring temperature of −15 °C, water droplet could not slid away completely from the surface, as shown in Figure S3(f). This result could be interpreted by the temperature dependence of the superhydrophobicity of a surface [24, 31]. The ZnO/PDMS composite maintained its superhydrophobicity at room temperature or when temperature was slightly decreased, i.e., −5 and −10 °C. However, when temperature is obviously decreased to −15 °C, its superhydrophobicity could be immediately changed. In other words, the CA could decrease and the SA could increase. Table 1 shows the dependence of CAs and SAs of the sample surface on temperature. One can see that the sample is still superhydrophobic at −5 °C, with a surface CA of 157° and a SA of 7.7°. However, the CA decreases to about 126° and 78° at −10 and −15 °C, respectively. In addition, the SAs are also very high (see Table 1). As a result, water droplet could not roll away readily from the tilted surface. However, even at a low temperature of −15 °C, only a small amount of ice accretion could be observed on the ZnO/PDMS surface [Figure S3(f)]. The icing delay time of the sample surface at different temperature and different tilting angle was tested and is shown in Table 2. As can be seen, water droplets did not freeze on the ZnO/PDMS sample surface at −5 °C even after a measuring time of 2 h. The horizontal surface still possessed a high icing delay time of about 1380 s at −10 °C, and the tilted surface can prevent water from freezing for 2 h. While at the measuring temperature of −15 °C, water freezing could not be prevented on the surface. However, the icing delay time increases apparently, which is about 210 s for the horizontal surface and 870 s for the tilted surface.

One major shortcoming of the superhydrophobic surfaces which hindered their practical applications is the bad mechanical stability. Mechanical contact with the surface either destroyed the fragile microstructures or peeled off the surface modifying agent, both of which can lead to the degradation of the superhydrophobicity [31, 32]. However, our superhydrophobic ZnO/PDMS surface was prepared by abrading with sandpaper, which means that the surface is robust against abrasion [25, 26]. In addition, an alternative method to resolve the aging problem of the superhydrophobic surfaces is to endow their recoverability when the superhydrophobicity of the surface is degraded under severe conditions, such as oil fouling. Fortunately, our preparation method of the superhydrophobic ZnO/PDMS surface is so simple that the damaged position of the surface could be easily recovered with few minutes using sandpaper. Figure 9 illustrates the recoverability of the superhydrophobic ZnO/PDMS surface. As shown in Fig. 9a, the right position of the superhydrophobic surface was deliberately damaged by using a knife and then the CA for water is lower than 150°. When the sample was slightly tilted (Fig. 9b), water droplet rolled away quickly from the undamaged positions, while stuck to the damaged position. The water droplet firmly adhered to the damaged

Table 1 CA and SA measurements for the ZnO/PDMS composite surface at different temperature

	−5 °C	−10 °C	−15 °C
CA	157.2° ± 2.2°	126.3° ± 2.4°	78.4° ± 3.2°
SA	7.7° ± 1.7°	None	None

Table 2 Icing delay time for the ZnO/PDMS composite surface at different temperature and different tilting angle

(°C)	Horizontal surface	Tilted surface
−5	>1800 s	>1800 s
−10	1380 ± 30 s	>1800 s
−15	210 ± 25 s	870 ± 42 s

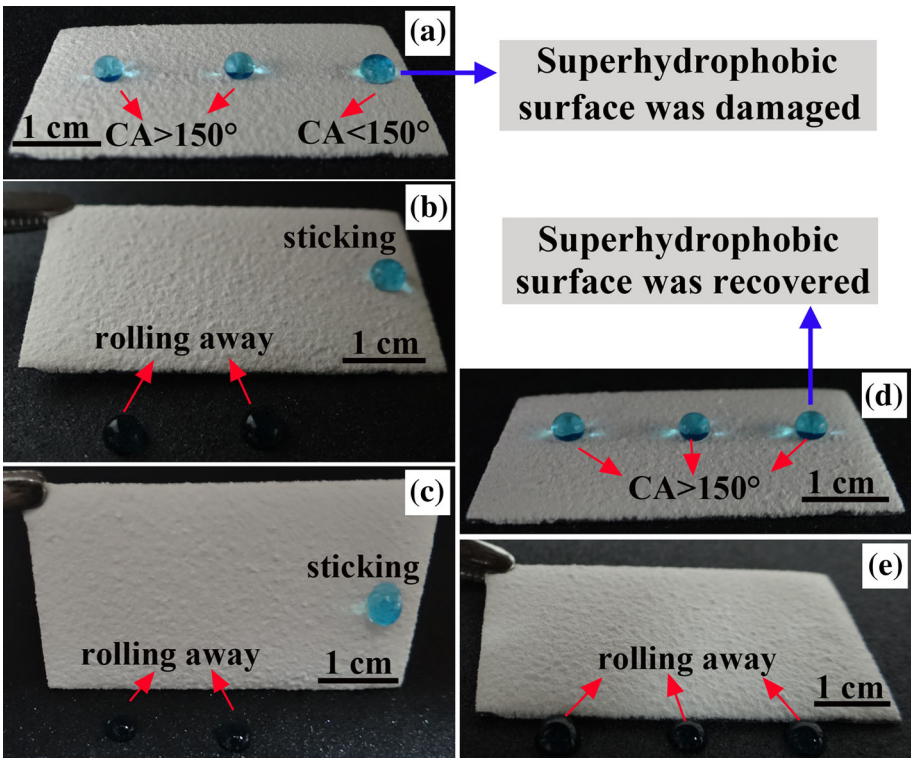

Fig. 9 Recoverability of the superhydrophobic ZnO/PDMS coating

position even when the surface was vertically placed (Fig. 9c). However, after a simple and short repair process, the sample recovered its superhydrophobicity (Fig. 9d). Water droplet showed a CA larger than 150° (Fig. 9d), and the easy-to-roll properties were also renewed (Fig. 9e).

Moreover, at extremely condensing conditions (e.g., very low temperature), water droplets will freeze and the formed ice in the cavities of the superhydrophobic surface could suppress the protrusions and grooves, which causes the damage of the surface rough structures of a superhydrophobic surface. As a result, the surface superhydrophobicity could be immediately changed after ice melting. Therefore, the stability against icing/deicing cycles for a superhydrophobic surface is also a critical parameter in determining the practical application of its anti-icing performance. Hence, a freezing test was carried out to investigate the stability of the superhydrophobic ZnO/PDMS composite coating. A piece of ZnO/PDMS composite coating was immersed in deionized water and placed in a cryogenic refrigerator at −20 °C overnight. Then, the sample was taken out and placed at ambient temperature until the ice completely melts. Afterward, the CA and SA of the sample were measured. Figure 10 shows the variations of CA and SA of the sample after different increasing freezing and thawing cycles (FTC). It could be observed that the CA slightly decreases with the increase in FTC. After 20 FTC, the sample still exhibits a CA larger

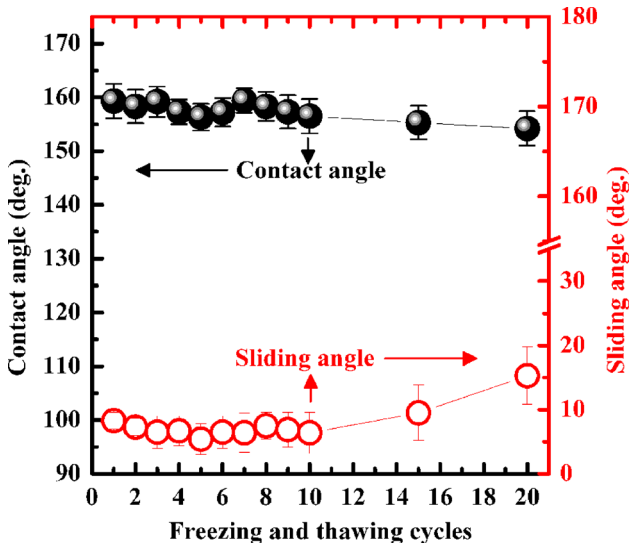

Fig. 10 Stability of the superhydrophobic ZnO/PDMS coating after freezing and thawing cycles

than 150°. In addition, the variations of SA after 10 FTC are not conspicuous. The robust stability of the superhydrophobic ZnO/PDMS composite could be interpreted by the elastic feature of the PDMS-based composite. It will be compressed through elastic deformation when loaded with external force. Once the external force is withdrawn, it will recover its original shape [33]. However, the SA is more than 10° after 15 FTC and even more than 15° after 20

FTC, which indicated the degradation of the superhydrophobicity. But it does not matter because the degraded superhydrophobicity could be easily renewed by a simple abrading process (see Fig. 9).

In summary, superhydrophobic surface of ZnO/PDMS composite coating based on DT-modified ZnO particles and PDMS matrix was fabricated via a simple surface abrading method. The as-prepared ZnO/PDMS composite coating possesses a high water CA of 159.5° and a low water SA of 8.3°. The anti-icing properties of ZnO/PDMS composite coating were investigated using a home-made apparatus. The influence of temperature and tilting angle of the surface on the icing behaviors of pre-cooled water droplet on the superhydrophobic surface was systematically studied. The results indicated that water accumulation on the horizontally placed superhydrophobic surface at all of the measuring temperatures from −5 to −15 °C could be reduced apparently because the dropping water merged together on the surface and subsequently slid away from the surface due to the continuous impinging of the dropping water. In addition, the tilted superhydrophobic surface exhibited excellent anti-icing properties at −10 and −5 °C because water droplet slid away from the surface very quickly without any residual due to the low SA of the superhydrophobic surface. Furthermore, the ice accretion on the tilted superhydrophobic surface could not be avoided completely at an even lower temperature of −15 °C. However, only a small amount of ice formed on the surface, which indicated that the tilted superhydrophobic surface could reduce ice accumulation remarkably at −15 °C. As a comparison, ice always accumulated on the pure Al surface, whether the surface is horizontally placed or inclined°. Moreover, the superhydrophobic possesses stability against 10 cycles of freezing and thawing which is also a critical characteristic for its practical uses. Importantly, once the surface microstructures of the ZnO/PDMS composite are damaged, it could be recovered easily. The preparation method of the superhydrophobic ZnO/PDMS composite coating could also be extended to other polymer-based composites, such as SiO_2/PDMS, TiO_2/PDMS, Al_2O_3/PDMS, ZnO/PMMA (polymethyl methacrylate) and $CaCO_3$/PS (polystyrene). Therefore, the above-mentioned superhydrophobic materials could be useful candidates for various icephobic/anti-icing applications in engineering materials, such as aircrafts and power lines.

Acknowledgments The work was supported by the National Natural Science Foundation of China (51263018 and 51463018), the S&T Supporting Plan of Jiangxi Province, Industrial Field (20133BBE50007), the xxx Basic Scientific Research Plan (A0520110xxx), and the S&T Supporting Plan of Jiangxi Province, Social Development Field (Grant No. 20122BBG70165).

References

1. Z.J. Zhang, X.L. Jiang, C.X. Sun, J.L. Hu, H.Z. Huang, D.W. Gao, Influence of insulator string positioning on AC icing flashover performance. IEEE Trans. Dielectr. Electr. Insul. **19**, 1335–1343 (2012)
2. X.Y. Li, B.B. Yang, Y.Q. Zhang, G.Q. Gu, M.M. Li, L.Q. Mao, A study on superhydrophobic coating in anti-icing of glass/porcelain insulator. J. Sol-Gel. Sci. Technol. **69**, 441–447 (2014)
3. S. Tarquini, C. Antonini, A. Amirfazli, M. Marengo, J. Palacios, Investigation of ice shedding properties of superhydrophobic coatings on helicopter blades. Cold Reg. Sci. Technol. **100**, 50–58 (2014)
4. C.Y. Peng, S.L. Xing, Z.Q. Yuan, J.Y. Xiao, C.Q. Wang, J.C. Zeng, Preparation and anti-icing of superhydrophobic PVDF coating on a wind turbine blade. Appl. Surf. Sci. **259**, 764–768 (2012)
5. A.G. Kraj, E.L. Bibeau, Phases of icing on wind turbine blades characterized by ice accumulation. Renew. Energy **35**, 966–972 (2010)
6. L.J. Chen, S.N. Chang, An approach of a HP for human factors analysis in the aircraft icing accident. Procedia Eng. **17**, 63–69 (2012)
7. Z.Q. Yuan, J.P. Bin, X. Wang, Q.L. Liu, D.J. Zhao, H. Chen, H.Y. Jiang, Preparation and anti-icing property of a lotus-leaf-like superhydrophobic low-density polyethylene coating with low sliding angle. Polym. Eng. Sci. **52**, 2310–2315 (2012)
8. P. Guo, M.X. Wen, L. Wang, Y.M. Zheng, Strong anti-ice ability of nanohairs over microratchet structures. Nanoscale **6**, 3917–3920 (2014)
9. M. Ruan, W. Li, B.S. Wang, B.W. Deng, F.M. Ma, Z.L. Yu, Preparation and anti-icing behavior of superhydrophobic surfaces on aluminum alloy substrates. Langmuir **29**, 8482–8491 (2013)
10. P. Kim, T.S. Wong, J. Alvarenga, M.J. Kreder, W.E. Adorno-Martinez, J. Aizenberg, Liquid-infused nanostructured surfaces with extreme anti-ice and anti-frost performance. ACS Nano **6**, 6569–6577 (2012)
11. Y. Wang, N.E. Hudson, R.A. Pethrick, C.J. Schaschke, Poly(-acrylic acid)–poly(vinyl pyrrolidone)-thickened water/glycol de-icing fluids. Cold Reg. Sci. Technol. **10**, 24–30 (2014)
12. B.J. Murray, S.L. Broadley, G.J. Morris, Supercooling of water droplets in jet aviation fuel. Fuel **90**, 433–435 (2011)
13. H. Wang, G.G. He, Q.Q. Tian, Effects of nano-fluorocarbon coating on icing. Appl. Surf. Sci. **258**, 7219–7224 (2012)
14. W. Barthlott, C. Neinhuis, Purity of the sacred lotus, or escape from contamination in biological surfaces. Planta **202**, 1–8 (1997)
15. P.F. Hao, C.J. Lv, X.W. Zhang, Freezing of sessile water droplets on surfaces with various roughness, and wettability. Appl. Phys. Lett. **104**, 161609-1–161609-5 (2014)
16. M.X. Wen, L. Wang, M.Q. Zhang, L. Jiang, Y.M. Zheng, Antifogging and icing-delay properties of composite micro- and nanostructured surfaces. ACS Appl. Mater. Interfaces **6**, 3963–3968 (2014)
17. L. Feng, Z.Y. Zhang, Z.H. Mai, Y.M. Ma, B.Q. Liu, L. Jiang, D.B. Zhu, A super-hydrophobic and super-oleophilic coating mesh film for the separation of oil and water. Angew. Chem. Int. Ed. **43**, 2012–2014 (2004)
18. B. Bhushan, Y.C. Jung, Natural and biomimetic artificial surfaces for superhydrophobicity, self-cleaning, low adhesion, and drag reduction. Prog. Mater Sci. **56**, 1–108 (2011)
19. T.L. Sun, G.Y. Qing, B.L. Su, L. Jiang, Functional biointerface materials inspired from nature. Chem. Soc. Rev. **40**, 2909–2921 (2011)
20. C.L. Jiang, W. Li, A facile method for preparations of micro-nanotextured Co_3O_4 films with the excellent superhydrophobic and anti-icing behavior. Mater. Lett. **122**, 133–138 (2014)

21. T.V. Charpentier, A. Neville, P. Millner, R.W. Hewson, A. Morina, Development of anti-icing materials by chemical tailoring of hydrophobic textured metallic surfaces. J. Colloid Interface Sci. **394**, 539–544 (2013)
22. L.L. Cao, A.K. Jones, V.K. Sikka, J.Z. Wu, D. Gao, Anti-icing superhydrophobic coatings. Langmuir **25**, 12444–12448 (2009)
23. L. Wang, M.X. Wen, M.Q. Zhang, L. Jiang, Y.M. Zheng, Icephobic gummed tape with nano-cones on microspheres. J. Mater. Chem. A **2**, 3312–3316 (2014)
24. Y.Y. Wang, J. Xue, Q.J. Wang, Q.M. Chen, J.F. Ding, Verification of icephobic/anti-icing properties of a superhydrophobic surface. ACS Appl. Mater. Interfaces **5**, 3370–3381 (2013)
25. F.J. Wang, C.Q. Li, Z.S. Tan, W. Li, J.F. Ou, M.S. Xue, PVDF surfaces with stable superhydrophobicity. Surf. Coat. Technol. **222**, 55–61 (2013)
26. M.A. Nilsson, R.J. Daniello, J.P. Rothstein, A novel and inexpensive technique for creating superhydrophobic surfaces using Teflon and sandpaper. J. Phys. D Appl. Phys. **43**, 045301-1–045301-5 (2010)
27. Q.P. Ke, W.Q. Fu, H.L. Jin, L. Zhang, T.D. Tang, J.F. Zhang, Fabrication of mechanically robust superhydrophobic surfaces based on silica micro-nanoparticles and polydimethylsiloxane. Surf. Coat. Technol. **205**, 4910–4914 (2011)
28. Y.Q. Qing, Y.S. Zheng, C.B. Hu, Y. Wang, Y. He, Y. Gong, Q. Mo, Facile approach in fabricating superhydrophobic ZnO/polystyrene nanocomposite coating. Appl. Surf. Sci. **285**, 583–587 (2013)
29. A.B.D. Cassie, S. Baxter, Wettability of porous surfaces. Trans. Faraday Soc. **40**, 546–551 (1944)
30. H. Zhang, X.F. Zeng, Y.F. Gao, F. Shi, P.Y. Zhang, J.F. Chen, A facile method to prepare superhydrophobic coatings by calcium carbonate. Ind. Eng. Chem. Res. **50**, 3089–3094 (2011)
31. L. Yin, Q.J. Wang, J. Xue, J.F. Ding, Q.M. Chen, Stability of superhydrophobicity of lotus leaf under extreme humidity. Chem. Lett. **39**, 816–817 (2010)
32. X.T. Zhu, Z.Z. Zhang, X.H. Men, J. Yang, K. Wang, X.H. Xu, X.Y. Zhou, Q.J. Xue, Robust superhydrophobic surfaces with mechanical durability and easy Repairability. J. Mater. Chem. **21**, 15793–15797 (2011)
33. C.H. Su, Y.Q. Xu, F. Gong, F.S. Wang, C.F. Li, The abrasion resistance of a superhydrophobic surface comprised of polyurethane elastomer. Soft Matter **6**, 6068–6071 (2010)